Cite this article
Hay S, Weidlich I, Wolf I and Villalobos FA (2022)
Pipe axial displacements from a monitored pipeline connected to a district heating network.
Proceedings of the Institution of Civil Engineers – Energy **175(3)**: 150–161,
https://doi.org/10.1680/jener.21.00100

Research Article
Paper 2100100
Received 26/08/2021;
Accepted 16/11/2021;
Published online 04/01/2022

Energy

ice Publishing

Pipe axial displacements from a monitored pipeline connected to a district heating network

Stefan Hay Dipl.-Ing.
Project Manager and Scientific Instructor in District Heating, Cooling and Combine Heating and Power (CHP), Research and Development, AGFW, Frankfurt am Main, Germany

Ingo Weidlich Dr.-Ing.
University Professor, Infrastructural Engineering, HafenCity University Hamburg, Hamburg, Germany

Ingo Wolf Dipl.-Ing.
Quality Assurance and Standardization Consultant, Colmarer Straße 1, Bremen, Germany; formerly at enercity Netz GmbH, Hannover

Felipe A. Villalobos CEng, MSc, DPhil
Assistant Professor, Department of Civil Engineering, Universidad Católica de la Santísima Concepción, Concepción, Chile
(Orcid:0000-0002-5419-3958) (corresponding author: avillalobos@ucsc.cl)

The development of a monitored district heating piping system has allowed the study of axial displacement variations in a buried pipeline. This piping system includes four instrumented sections of piping within an in use district heating network. There are also different conditions under testing such as thickness of expansion cushions, temperature ranges and bedding soil types. The pipe axial displacements were on-line monitored by means of extensometers in six positions along each of the four sections of the pipeline. Measured maximum pipe axial displacements were 24 and 25 mm in the corners of the 41 m long monitored pipelines, while estimated values were 23 mm using current recommendation procedures and 27 mm using calibrated commercial computer programs. One temperature unloading–reloading caused displacements to not return to the same values as before, but around 3 mm smaller. Therefore, several unloading–reloading temperature cycles may affect the pipe deformation behaviour in the short and long term.

Keywords: district heating/field testing & monitoring/pipes & pipelines

Notation

A_s	cross-section area
D_a	pre-insulated pipe external diameter
d_a	external steel pipe diameter
E	steel elastic modulus
F_{el}	elastic reaction force of the soil
F_G	weight force of the steel pipe and water inside
F_N	normal forces applied on the pipe
F_p	force along the pipe
F_R	frictional force between the pipe and the soil
h	soil depth on pipe crown
K_0	coefficient of earth pressure at rest
L	length of pipe section
p	internal fluid pressure
RD	soil relative density
r_m, r_i	average and inside radius of the steel pipe
T	temperature
T_0	initial temperature
t	steel pipe thickness
t_c	PE-casing thickness
t_f	foam thickness
t_t	cushion thickness
u	pipe displacement
z	depth
α_T	coefficient of thermal expansion
γ	soil unit weight
γ_{steel}	steel unit weight
γ_w	water unit weight
ΔT	temperature increment
δ'_{res}	residual soil–pipe angle of friction
ε	pipe strain
ε_T, ε_σ	pipe strain due to temperature and due to stress
μ	coefficient of friction
ν	steel Poisson's ratio
σ_0	stress around the middle of the pipe
ϕ'_{res}	residual soil angle of friction

1. Introduction

District heating is an energy system for the generation and distribution of large amounts of heat which is considered as one of the most efficient and sustainable engineering solutions to meet the heating demand and capable to reduce greenhouse gas emissions (e.g. Frederiksen and Werner, 2013; Laajalehto *et al.*, 2014; Werner, 2017). Integration of renewables is one of the current challenges – that is, the use of solar or geothermal

instead of fossil fuels (e.g. Lund *et al.*, 2014). District heating systems transport heat from a central plant to residential, commercial and industrial users by means of extensive pipeline networks. Consequently, district heating distribution relies significantly on the pipeline network. The most widely used laying system corresponds to a pre-insulated pipeline (CEN, 2020a). The pipes consist of a steel service pipe covered with polyurethane (PUR) and an outer casing of polyethylene (PE), which are joined using special welding technologies developed for reducing heat losses and protecting the pipes from failure. Nonetheless, since the buried and pre-insulated pipes carry a hot fluid under high-pressure levels, large temperature variations in the steel pipes can cause significant pipe deformations, resulting in complex interactions between the moving pipe and the adjacent soil. Excessive pipe deformations can lead to serviceability problems such as leakage or pressure reductions and ultimately pipe or joint breakage that could eventually stop the energy supply. Therefore, the study of the soil–pipe interaction phenomenon in district heating requires on one hand the analysis of forces and displacements in the pipe due to fluid temperature changes and on the other, knowledge of relevant soil physical properties. For that reason, in addition to the pipe physical properties, geometry and burial depth, it is necessary to know the pressure and temperature changes of the fluid as well as the soil relevant characteristics such as grain sizes, water content, density, strength and stiffness.

Researchers have mostly studied pipe–soil interaction experimentally at a small scale in the laboratory (Achmus and Weidlich, 2016; Weidlich, 2008; Weidlich and Achmus, 2008) and using numerical analysis (Achmus, 1995; Achmus and Rizkallah, 1997; Gerlach and Achmus, 2017). Previous measurements in the field have been limited to the test of a fluidised soil as a trench fill for a district heating pipeline (AGFW, 2017). Consequently, it is worth pointing out that currently there is a lack of information related to measured pipe axial displacement distributions along pipelines in real operating district heating conditions. On the grounds that there is no systematic information available, a monitoring system in an operating district heating pipeline network has been developed for research purposes in Chemnitz, Germany (Hay *et al.*, 2018; Villalobos *et al.*, 2018, 2019). This on-line monitoring system was implemented with a control unit that regulates the temperature and fluid pressure supplied to the studied pipeline. The novelty and challenge of this research project is the systematic data recording which is first of its kind in district heating. This research project offers the unprecedented opportunity to compare real-time experimental results with current design guidelines and calculation procedures from analytical and commercial computer programs. This is important for the validation of current design practice, which allows knowing the actual design scopes and restrictions as well as possible improvements needed. Especially, the effect of temperature-induced loads on buried pipes which need elongation measurements in real conditions in order to assess appropriately the pipe performance with time. This validation can provide more confidence in the application of the soil–pipe interaction physical–mathematical model adopted in the design codes. The lack of monitoring data in real operational conditions may let in an uncertain situation for the current calculation framework, hence, less confidence in its use. Moreover, professionals directly and indirectly involved in the design, construction and maintenance of district heating pipeline networks will be benefited from this research study. Furthermore, owners of district heating networks need to assess accurately the performance of pipelines to be able to take the right decisions related to operational maintenance, remaining life time and replacement.

The design and construction of district heating pipelines follow well-established procedures to assess pipe forces and displacements according to standards and recommendations (e.g. AGFW, 2021; CEN, 2019). However, calculation procedures require data from field measurements to validate their use. In general, the available high-quality data of field measurements of pipe axial displacement are scarce and in district heating applications there are only a few (AGFW, 2017; Hay *et al.*, 2018; Villalobos *et al.*, 2019). Therefore, measured results from pipe axial displacements will allow the comparison with theoretical estimations. This study follows closely the work of Hay *et al.* (2018) and Villalobos *et al.* (2019), where the monitored district heating pipeline system is described and part of the results of temperature and earth pressure distributions around the pipeline are presented and analysed as well as some of the pipe axial displacements. In this study, high-quality instrumented buried pre-insulated pipelines for the measurements of displacements under temperature-controlled conditions are described. The measurement of axial displacements of buried pipes using 24 extensometers is described and the results are studied during specific moments and conditions. Moreover, theoretical calculations are carried out to estimate the pipe axial displacement, which are compared with the measured data.

2. Design and construction of the monitored pipeline

The design of the pipeline for the monitoring district heating piping system was based on the recommendations of CEN (2019) and AGFW (2021). Table 1 summarises the parameter values used in the design of the pipeline. These values of temperature, pressure and soil conditions are not necessarily the same to be found in the field under operational conditions, since they are mostly based on experience and design standards for unfavourable soil, pressure and temperature conditions. For that reason, these values provide an upper bound

Table 1. Measured, calculated and recommended parameter values used in the design of the district heating monitored pipeline

Component	Parameter: unit	Value	Comment
Fluid	Maximum operation temperature, T: °C	135	Recommended
	Installation temperature, T_0: °C	10	Recommended
	Maximum internal fluid pressure, p: bar	25	Recommended
Steel pipe	Elastic modulus, E: MPa	206 290	Calculated
	Thermal expansion coefficient, α_T: 1/K	1.24×10^{-5}	Calculated
Soil	Depth above the pipe crown, h: m	0.80	Measured
	Unit weight, γ: kN/m^3	19.0	Measured
	Angle of internal friction, ϕ: °	32.5	Recommended
	Soil-casing angle of interface friction, δ: °	21.8	Recommended
	Friction coefficient, μ	0.4	Recommended
Pre-insulated pipe	Displacement in the corner, u: mm	56	Calculated
	Friction force, F_R: kN/m	5.1	Calculated
Steel pipe	Axial compression stress: MPa	82.8	Calculated
	Axial compression stress: MPa	184	Allowable
PUR insulation	Shear stress: kPa	10	Calculated
	Shear stress: kPa	27	Allowable
	Compression stress: kPa	18	Calculated
	Compression stress: kPa	150	Allowable

Recommended: standard value normally adopted for design in the district heating industry based on EN 13941 (CEN, 2019) and AGFW (2021)

compared for instance with the axial displacements measured in the monitored pipeline.

The design, construction and operation of the instrumented pipeline have been already reported (Hay *et al.*, 2018; Villalobos *et al.*, 2019). Briefly, the pipeline is 194 m long divided into two parallel supply and return parts, which in turn is further divided in four sections, as shown in Figure 1. The four different sections allow the assessment of various combinations of materials such as type and amount of sleeves in the joints, soil beddings as well as with or without expansion cushions at the pipeline corners. Figure 1 illustrates the instrumented pipeline with the four 41 m sections plus 5 m of perpendicular pipe connecting to the fixed points. For the installation of similar sections of pipes and to restrict pipe movements, six reinforced-concrete blocks were used as fixed positions; namely two in each extreme and two in the middle of the monitored pipelines as shown in Figure 1. Also shown in Figure 1 in section 3 are the extensometer positions with a number that indicates the distance from the shaft centre. The location of four temperature sensors to measure the fluid temperature is also indicated with the letter T in Figure 1. Figure 2 shows the A–A cross-section in sections 2 and 4, showing also the plastic box for fixing the extensometers. Table 2 summarises each section in term of joint type, number of joints and soil bedding. Shrink-on sleeve is a type of joint normally carried out which results in a joint diameter larger than that of the pre-insulated pipe. Extruded sleeve is another

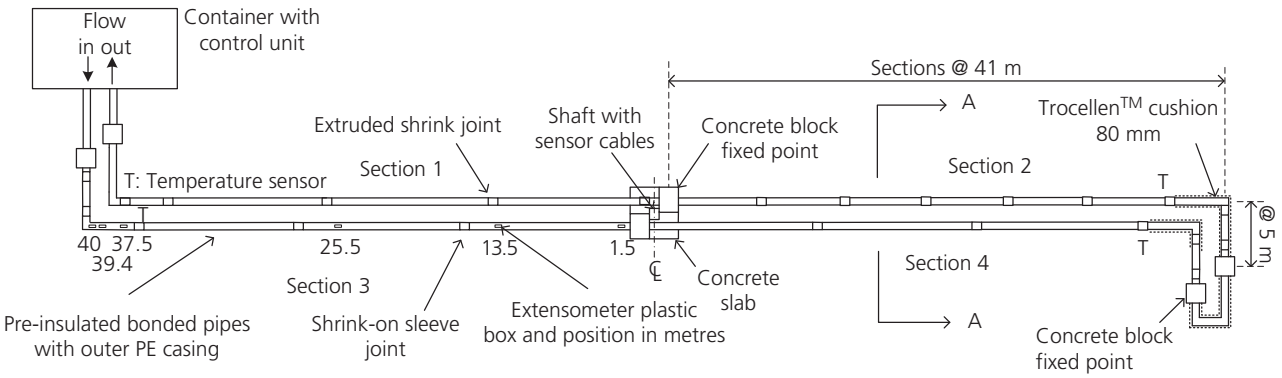

Figure 1. Sketch of the monitored pipeline sections, showing control unit, fixed points, joints, cushions, temperature sensors and extensometer positions in metres from the shaft centre line

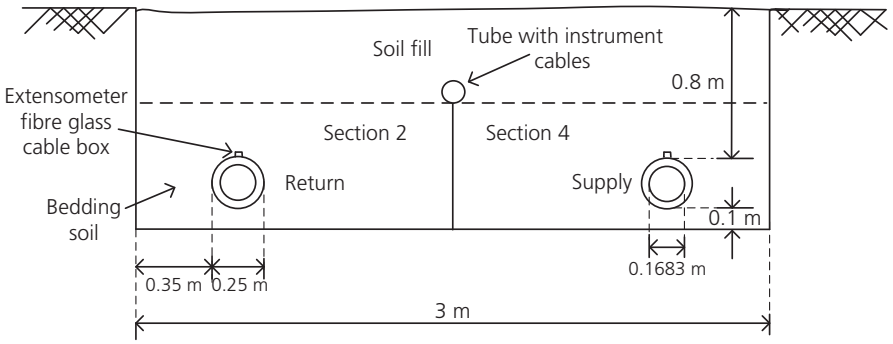

Figure 2. Trench A–A cross-section with pipes of sections 2 and 4 showing the extensometer position on the pipes' crown

Table 2. Description of the pipeline sections

Section	Joint type	Number of joints	Soil bedding
1	Extruded shrink	5	Medium–fine sand
2	Plastic shrink-on sleeve	8	Medium–fine sand
3	Plastic shrink-on sleeve	5	Medium–fine sand
4	Plastic shrink-on sleeve	5	Medium–coarse sand with fine gravel

Source: Hay *et al*. (2018), Villalobos *et al*. (2019)

type of joint not so often used which require a special machine that make a finishing with almost the same diameter of the pre-insulated pipe.

There is no foam in the last sleeve next to the corner with the idea to assess the relative displacement between the casing and the medium steel pipe.

The tested pre-insulated bonded pipes correspond to a DN 150/250 pipe (CEN, 2020a, 2020b), which are composed of a central medium steel pipe, PUR foam-covering insulation, external PE casing and at the pipeline corners Trocellen^{TM} cushions with the dimensions of diameters and thicknesses as shown in Figure 3. The use of cushions attempts to reduce the soil–pipe interface friction at the pipeline corners and therefore allowing larger displacements to occur.

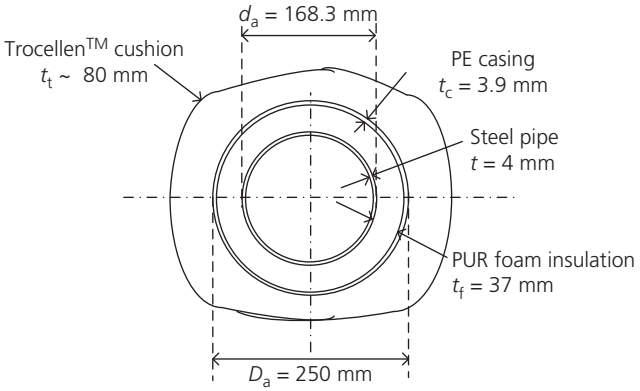

Figure 3. Cross-section of a district heating pipe DN 150/250 (CEN, 2020a) used in the investigation

3. Monitoring axial displacements

Extensometers are normally used for measuring tunnel convergence and subsidence as well as foundation settlements and in general for measuring displacements of structures usually in pre-excavated boreholes in soil or rock. The displacement is obtained by measuring the change of distance between two points using a fibre glass rod inside a plastic tube. When one extreme is fixed, the displacement measured becomes absolute and not relative. In this form, several points can be measured to obtain displacement variations along a pipe (Dunnicliff, 2012). Reported applications of extensometers in tunnel, pile and wall projects can be found, for example, in Kavvadas (2003), Burd *et al*. (2020) and Vulliet *et al*. (1997). However, in district heating pipeline applications, the use of extensometers is relatively new and with only a few available data published (AGFW, 2017).

Four sets of six fibreglass extensometers Glötzl GKTE 16 (Rheinstetten, Germany) were used for the measurement of

axial displacements along six positions of the buried pre-insulated pipes. The total 24 extensometers (12 in the supply and 12 in the return pipeline) are positioned at the same distance with respect to the shaft centre to be able to compare results. This extensometer is a versatile and compact unit that provides reliable results whose measurement length can span from 0.5 up to 100 m with a measurement range between ± 30 and ± 125 mm. The measurement accuracy depends on the measurement length, so for a length of 13.5 m the accuracy is ± 0.003 mm and for 40 m is ± 0.075 mm (Glötzl, 2007). The 24 extensometers were calibrated by Glötzl between November 2016 and April 2017. The calibration range was 100 mm (+80 mm and −20 mm) with a clear linear relationship resulting in a calibration factor of 0.16 mA/mm.

Figure 4(a) shows an extensometer in a plastic box in a 12:00 h position covered by the cushion close to the corner, where the glass fibre cable is fixed to measure the pipe displacement in this position. Figure 4(b) shows the extensometer installed in a joint directly on the steel pipe using a steel plate also in a 12:00 h position. Later on, the joint is filled with mineral wool for insulation and to prevent direct contact

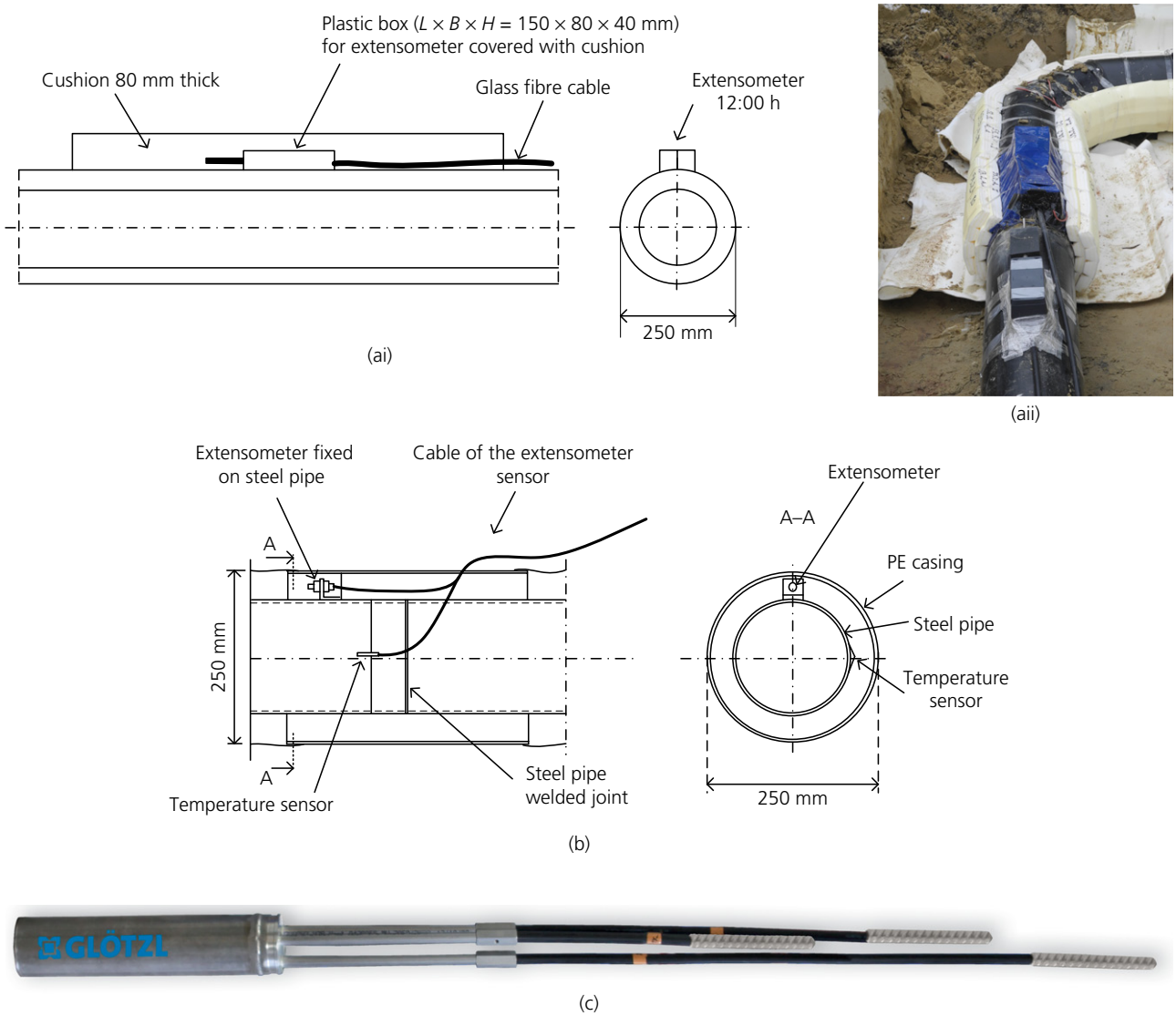

Figure 4. (a) Sketch and photograph from section 3 of the extensometer installed on the pipe casing and covered by the cushion; (b) extensometer and temperature sensor installed on the steel pipe at 12:00 and 15:00 h positions and (c) Glötzl fibreglass rod extensometer GKTE 16 (Glötzl, 2007)

between the steel medium pipe and the PE casing. The cushion and the foam over the extensometers significantly reduce the soil shearing on the instrument and hence avoiding to have effects on the measured displacements. This four series of six sensors as well as the signal converter are installed in the concrete control shaft right in the middle as shown in Figures 1 and 6. A photograph of a three fibreglass extensometer is shown in Figure 4(c).

In addition, four temperature sensors were used to measure the fluid temperature as shown in Figure 4(b), whose location in the pipeline is shown in Figure 1 with the letter T. The sensors correspond to Ni1000 TK5000 with sealed cables IP68, which can measure in the range of −50 to 180°C.

In the four sections, the last joint before the corners is initially not foamed because in that space sensors are installed.

(a)

(b)

Figure 5. (a) Open trench with both pipes crossing the concrete blocks and extensometers attached inside plastic boxes on the pipes' crown (section 1 on the right and section 3 on the left) and (b) extensometer cables connected to the shaft

The copper and glass fibre cables run along the openings left in the foam, which were sealed later on. Figures 5(a) and 5(b) show the open trench during the construction and installation of instruments with both pipes and the extensometers fixed in plastic boxes on the pipes with the cables towards the connection in the shaft.

4. Shaft

The extensometers cabled to the shaft were conducted to the control unit by a tube as illustrated in Figure 6, where signal recordings are stored and sent outside through wireless internet. Figure 6 depicts a view from above of the shaft where the extensometer cables are plugged in. This figure also shows the pipe sections, concrete slab and the concrete blocks. From the shaft, data cables are buried along the piping trench to the control unit where the data are received and recorded.

5. Analysis of pipe axial displacements

As shown in Figure 1, the position of the six extensometers along each section was at 1.5, 13.5, 25.5, 37.5, 39.4 and 40 m from the concrete shaft in the middle. The extensometers were installed at the crown of the pipes for the comparison of displacements at the same level. The extensometers at 37.5, 39.4 and 40 m started recording displacements immediately after the initial filling of the pipeline with fluid temperature up to around 56°C, recording displacement values in the order of 5 and 6 mm, while the other sensors recorded no pipe movement whatsoever. Once the filling process was completed after 97 min, the pump was switched on to generate a flow with a target fluid temperature of 90°C. Figure 7 shows the variation

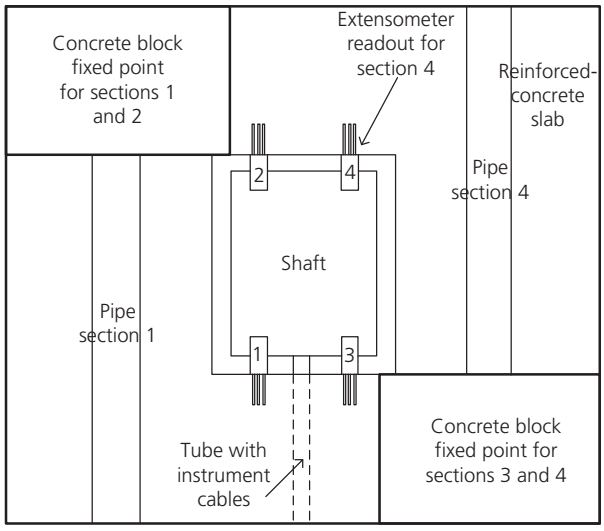

Figure 6. View from above of the shaft in the middle showing the pipe sections, instrument cables, concrete blocks and cable connection points for extensometers coming from each section

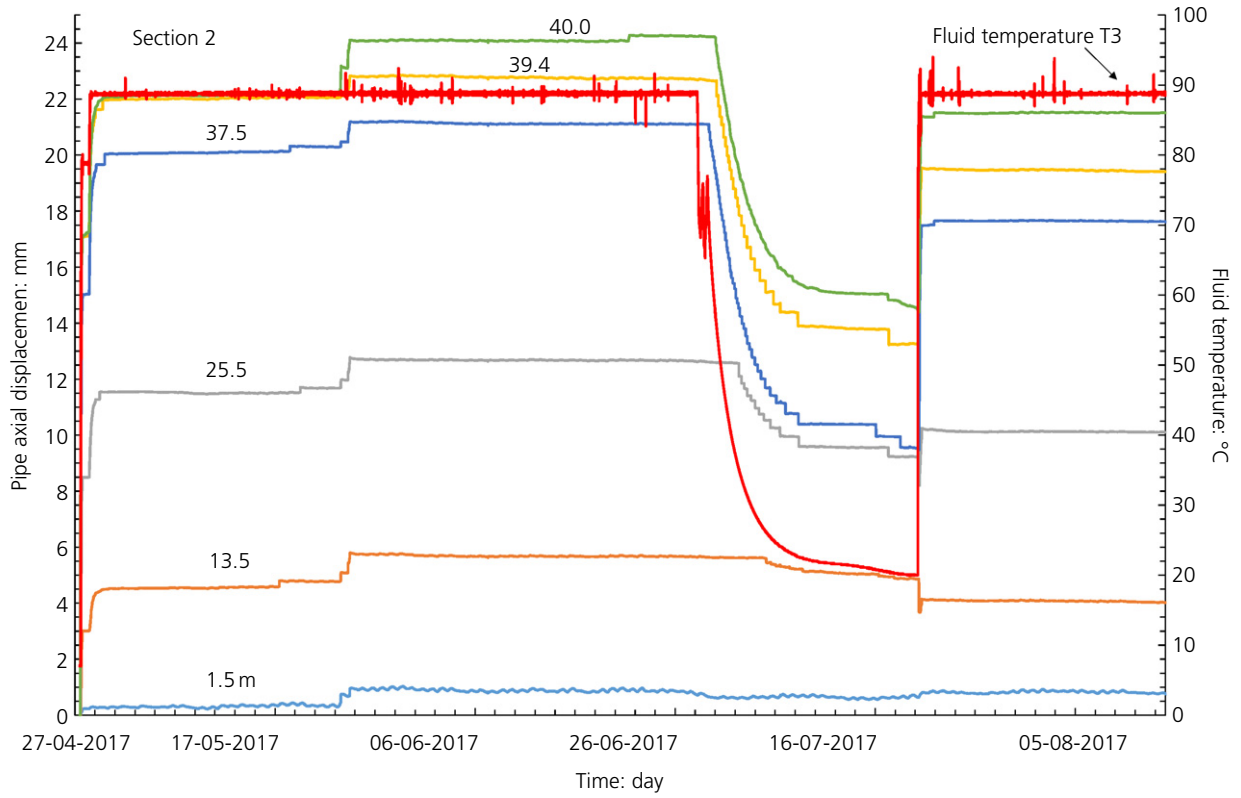

Figure 7. Variation with time and medium temperature of pipe axial displacements measured on the casing in the return section 2 for six positions at 1.5, 13.5, 25.5, 37.5, 39.4 and 40 m from the shaft in the centre

with time and temperature of the pipe axial displacement in the six positions along the pipe in the return section 2. It can be observed that once the fluid temperature increased from 8 to 78°C in approximately 3 h, the pipe moved axially towards the corner with maximum displacements at the corner between 15 and 17 mm in one day. At 25.5 and 13.5 m displacement values of 8.4 and 3 mm were recorded, respectively, while at 1.5 m practically no movement was recorded. After 3 days with a constant temperature of 89°C, steady higher values of displacements were reached, namely 0.3, 4.5, 11.5, 20.1, 21.9 and 22.1 mm, respectively. After a month under 89°C, steady values reached a plateau of maximum displacements of 1, 5.8, 12.7, 21.2, 22.8 and 24.1 mm, respectively.

These maximum values stayed almost constant for another 2 months until the temperature descended from 89 to 20°C in 22 days as it can be observed in Figure 7. As a result, pipe axial displacements decreased to 0.6, 4.9, 9.2, 9.6, 13.2 and 14.7 mm, respectively. Once the temperature returned to the previous 89°C, the displacements did increase but to steady values below those recorded before (0.8, 4.0, 10.1, 17.6, 19.5, 21.5 mm). The irrecoverable deformation is believed to be mainly due to soil densification, which in turn increases friction in the soil–pipe interface restraining the pipe to come back exactly to the previous displacement values. A similar response was found in the supply section 3, although with slightly higher values at the corner (23.0 mm). It is clear that a first temperature unloading–reloading can have a significant effect on the pipe displacements. However, more monitoring time is needed in order to find out the long-term pipe response to temperature unloading–reloading cycles.

The axial displacement variation with time and temperature along the pipeline in the return sections 1 and 2 and the supply sections 3 and 4 are shown in Figures 8 and 9, respectively. These experimental results allow the comparison with displacement estimated from the current calculation methods as detailed in the Appendix (AGFW, 2021).

In Figures 8 and 9 the time is in days with hours in brackets when time is less than 1 day. These figures show displacements just after zeroing and during 3 months and a half (109 days). In addition, discontinuous lines from displacement calculations for loose and dense soil are included. The main soil and pipe

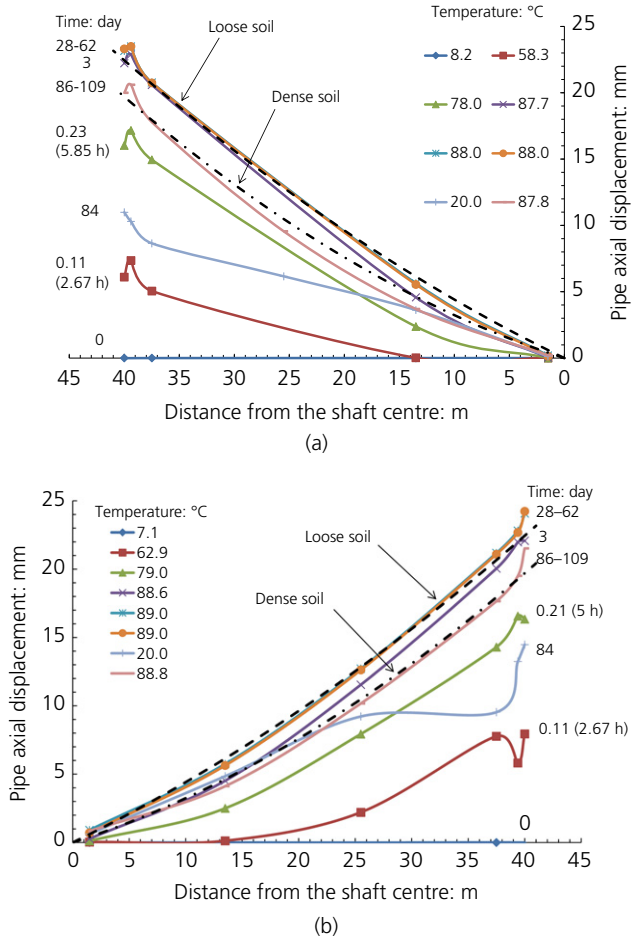

Figure 8. Measured and estimated pipe axial displacements along the pipe from the shaft centre 0 to the corner 40 m away in (a) section 1 and (b) section 2

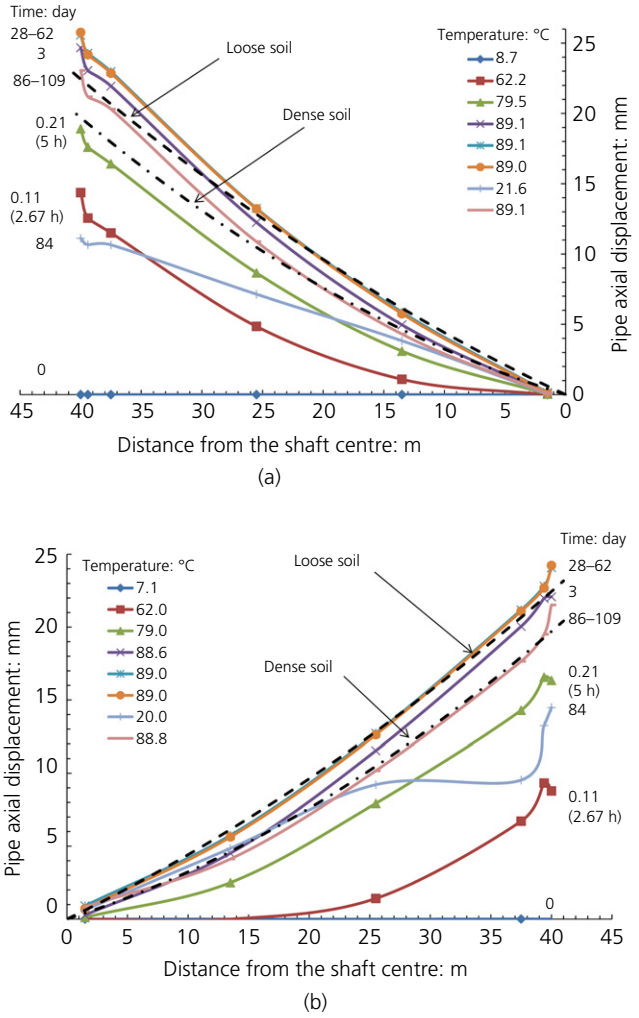

Figure 9. Pipe axial displacements along the pipe from the centre 0 to the corners 40 m away in (a) section 3 and (b) section 4

input data adopted are summarised in Tables 3 and 4. Loose soil data are based on the results from soil mechanics laboratory and in situ geotechnical tests (AGFW, 2020; Villalobos *et al.*, 2019). The coefficient of friction $\mu = \tan \delta$, where δ is the residual soil–pipe angle of friction, was determined in the laboratory from direct shear tests according to DIN (2002). For loose sand, δ was between 22.5 and 23.2°, which is a representative of the initial in situ conditions. For that reason a value of $\delta = 23°$ was adopted for the calculations, noting that it is close to the normally used relation of $\delta = 2/3\phi$, where ϕ is the soil angle of friction. From direct shear tests, ϕ was between 35.8 and 36.1°. These values represent the initial in situ conditions and are used in Figures 8 and 9 to estimate the pipe axial displacements.

The dense soil input values attempt to capture the effect of soil densification with time and aim mainly to obtain a range in which the calculation method is bounded. Section 4 has a coarser bedding material, however, the residual friction parameter values are almost similar to those in sections 1–3. The coefficient of friction for dense sand was obtained fitting

Table 3. Soil parameter values used in the calculation

Soil parameter and unit	Loose sand	Dense sand
Unit weight, γ: kN/m^3	15	17
Residual soil angle of friction, ϕ'_{res}: °	36	45
Coefficient of earth pressure at rest, K_0	0.41	0.29
Residual soil–pipe angle of friction, δ'_{res}: °	23	30
Coefficient of friction, μ	0.42	0.58
Relative density, RD: %	42	85

Table 4. Pipe parameter values adopted for pre-insulated steel pipes, fluid and operation conditions

Component	Parameter, unit	Value
Steel pipe	Unit weight, γ_{steel}: kN/m^3	78.5
	Elastic modulus, E: MPa	207 440
	Poisson's ratio, ν	0.3
	Coefficient of thermal expansion, α_T: 1/K	1.08×10^{-05}
Fluid	Water unit weight, γ_w: kN/m^3	9.8
	Internal fluid pressure, p: MPa	1.2
	Temperature increment, ΔT: K	82
Pre-insulated pipe	External steel pipe diameter, d_a: m	0.1683
	Steel pipe thickness, t: m	0.004
	Cross-section area, A_s: m^2	0.0021
	Pre-insulated pipe external diameter, D_a: m	0.25
	Length of pipe section, L: m	41
	Soil depth on pipe crown, h: m	0.8

the last curves of axial displacement for 86–109 days (after a 70°C temperature drop and 70°C back to reach 90°C again). The values in Table 4 are mainly based on the pipeline design and construction report by Wolf *et al*. (2016) and suggested values in AGFW (2021).

Figure 8(a) corresponds to pipe axial displacements in the return section 1, where it is clear to observe the increase of axial displacement along the pipe from the fixed middle point to the corner. Moreover, the position of the axial displacement curves depends on the temperature and time. Initially, 2.67 h after displacement zeroing and under a fluid temperature of 58.3°C, the pipeline displaces axially up to 7 mm on the corner. Once the fluid temperature is increased to 78°C after almost 6 h, axial displacements increase further up to 17 mm. When the temperature reaches 88°C, the pipe moves axially up to 23 mm and no major difference can be seen after 3, 28 or 62 days since these last two curves are almost merged. Then, it can be pointed out that a steady condition is achieved, where no further displacements occur.

Another feature of the displacement curves is that they show a much higher increase of axial displacement in the last points of measurement at 39.4 and 40 m. This is caused by the fact that in the last joint there is no foam insulation, which reduces the friction compared to the friction between PE casing and the bedding material. The idea behind was to determine the relative displacement between the casing and the steel pipe, which results to be between 1 and 1.5 mm. Moreover, this higher gradient of axial displacements in the area of expansion cushions (corners) may be caused by the lower friction value between PE casing and the expansion cushions (for Trocellen $\mu = 0.22$ (AGFW, 2021) compared to the friction value between PE casing and the adjacent bedding material ($\mu = 0.42$ and 0.58).

When the temperature diminishes to 20°C after 84 days, so does the displacement to values up to 11 mm. However, when the temperature returns to almost 88°C, displacements do not recover to the previous maximum values of 23 mm, instead they have values of up to 20.6 mm. This behaviour requires study for more cycles since this occurs in district heating pipelines over a period of several years (e.g. maintenance, winter–summer cycles).

Note that the calculated values of pipe axial displacement show a very good agreement for loose soil when a steady condition is reached at 28–62 days, except for the beginning and final 2 m where there is some difference. The dense soil assumption despite not being the initial condition on site, it shows a lower boundary for the displacement – that is, how low the displacement estimation can be.

Almost similar displacement variation patterns were found in section 2, as shown in Figure 8(b). Therefore, it is not possible to find a clear difference between the rough eight shrink-on sleeve joints of section 2 and the five smooth extruded sleeve joints of section 1, at least in the steady results between 28 and 62 days. In Figure 8(b) it is also clear to observe the steady increase of displacement from day 0 to 62 days. On day 84, a drop in temperature reduces the displacements creating a transient condition, which does not follow the same shape of displacement variation as in the previous sequences. In the last case, when temperature returns to 88.8°C, the displacement curve is again with the same convex parabolic shape as before, but with smaller displacement values at least in the positions away from the centre.

The estimated curve for loose soil matches almost exactly the experimental curves for 28 and 62 days, except the last 1 m where there is a higher increase rate at 40 m. Coincidently, the estimated curve for dense soil follows the trend of the experimental curve for 86 and 109 days, which is the reloading curve after the first unloading. This is an indication that soil densification took place and in turn the soil became stiffer.

Figure 9(a) shows that axial displacement variations in section 3 are relatively similar to those in section 2, although slightly higher values close to the corner and with a difference in the transient period when the temperature drops to 20°C. In fact, estimated axial displacements for loose soil in the first 25 m follow relatively well the experimental curves for 28–62 days. Notwithstanding, beyond 25 m the estimated curve deviates to lower values of axial displacement with a maximum difference of 3 mm at 40 m. Perhaps, this can be attributed to higher return fluid temperatures of around 1 or 2°C more than in sections 1 and 2 compared with the supplied fluid in section 3. The estimated curve for dense soil tends to initially follow the

reloading curve, but beyond 25 m underestimate the axial displacement.

Figure 9(b) shows that displacement variations in section 4 are similar to those of sections 1 and 2, with the only noticeable difference in the transient period when the temperature drops to 20°C. It is worth highlighting that the estimated curve for loose soil matches the experimental curves for 28–62 days almost all along the pipe, except at 40 m. A possible explanation was already pointed out related to the difference of interface friction in the corners between PE casing and cushion and PE casing and bedding material. A similar good match occurs for the estimated curve for dense soil and the experimental reloading curve. Apparently, the coarser sand in section 4 has no major effect on the axial displacement results. This is probably because the residual angles of internal and interface friction are almost the same. Moreover, the different types and number of joints in each section seem to not show a clear significant effect on the axial displacement results. Furthermore, when using the commercial software Rohr2 (2017) and sisKMR (2016) with the appropriate input data for the operation and soil conditions detailed in Tables 2 and 3 for loose sand, the results of maximum axial displacement with and without cushion are equal to 30 and 27 mm, respectively. These results are above the measured value, although they provide a fair approximation.

6. Final comments and conclusions

A sophisticated on-line monitoring system in an operating district heating pipeline network allows systematic data recording of high-quality measurements of axial displacements by means of extensometers and under fluid temperature-controlled conditions. The instrumented buried pipeline is the first of this type in district heating and it offers a unique opportunity to compare experimental results with current design guidelines and calculation procedures from analytical and commercial computer programs. Moreover, due to the flexibility and high accuracy and precision of results that can be obtained with this automatically controlled system, it can be adopted as a reference for testing different types of pipes, joints, cushions and soils.

The measured variation of axial displacements with time along the buried pipeline in loose soil showed a non-linear increase with length. After 28 days under continuous flow at 89°C, pipe axial displacements stabilised with maximum values between 23.5 and 25.8 mm (on steel) and between 22.5 and 24.6 mm (on the casing). An estimated maximum value of 22.4 mm compares relatively well with the above measured values. Commercial computer programs calculated 27 and 30 mm as a maximum axial displacement without and with cushion, respectively, values above the measured axial displacement, however, offered a fair estimation.

Since the estimations of axial displacement variations along the four pipe sections matched the measured values, it can be concluded that the calculation procedure adopted is able to properly estimate the axial displacements of buried pre-insulated pipes for district heating systems, allowing the use and choice of parameter values without pre-established values or relationships from standards as usually included in commercial computer programs.

When the temperature descended from 90 to 20°C during 22 days, the axial pipe displacements showed a transient response. Moreover, when the temperature was increased back again to 90°C pipe axial displacements were still unsteady and once stabilised they did not return to the same values as before, but around 3 mm smaller. This may be attributed to pipe–soil stiffening expressed as soil densification due to pipe expansion and contraction which compacts the surrounding soil. Cushions may also be compacted by increasing pipe–soil stiffness and friction. Therefore, further research is needed to study the unloading–reloading temperature cycles.

Acknowledgements

This study is part of ongoing research programmes on district heating by AGFW for the development and improvement of pipeline networks. The authors are especially grateful to the BMWi German Federal Ministry of Economics and Energy for the funding support to these ongoing research programmes (funding code 03ET13335). The last author especially acknowledges the funding granted by Zeit Stiftung by means of an academic Fellowship at HafenCity University as well as fund DIREG 04/2021 from the Office of Research (Dirección de Investigación) at the Universidad Católica de la Santísima Concepción.

Appendix

Expressions and calculation procedures used are according to part 10 of AGFW (2021). The friction force per metre along the pipe F_R is due to the normal forces applied on the pipe F_N and the weight of the steel pipe and water inside it F_G. Following Coulomb's friction law, the friction force results from a direct relation between a friction coefficient μ and the normal forces to the surface. It is a common practice to include the weight of the pipe and water in the calculations to obtain the maximum friction force.

1. $$F_R = \mu(F_N + F_G)$$

where

2. $$F_N = \sigma_0 \pi D_a \left(\frac{1 + K_0}{2}\right)$$

The stress σ_0 around the middle of the pipe can be estimated by

$$3. \quad \sigma_0 = \gamma z = \gamma\left(h + \frac{D_a}{2}\right)$$

where γ is the soil humid unit weight, h is the depth of the soil column above the pipe crown and D_a is the external diameter of the insulated pipe – that is, the steel pipe plus the foam and plastic mantle.

$$4. \quad F_G = 2\pi r_m t \gamma_{steel} + \pi r_i^2 \gamma_w$$

where t is the thickness of the steel pipe, γ_{steel} is the steel unit weight equal to 78.5 kN/m^3, γ_w is the water unit weight and r_m and r_i are the average and inside radius of the steel pipe.

$$5. \quad r_m = \frac{d_a - t}{2} \; r_i = \frac{d_a - 2t}{2}$$

Thus, replacing (2) and (4) into (1), results in

$$6. \quad F_R = \mu(F_N + F_G) = \mu\left[\sigma_0 \pi D_a \left(\frac{1 + K_0}{2}\right) + \left\{2\pi r_m t \gamma_{steel} + \pi r_i^2 \gamma_w\right\}\right]$$

The total axial strain $\varepsilon(x)$ in the pipe is the result of temperature increase and stresses applied on the pipe, for example, by the soil and fluid.

$$7. \quad \varepsilon(x) = \varepsilon_T + \varepsilon_\sigma$$

The strain due to a temperature change ΔT can be obtained by

$$8. \quad \varepsilon_T = \alpha_T \Delta T$$

where α_T is the coefficient of thermal expansion in 1/K, which for steel can be given by a function of the temperature T as

$$9. \quad \alpha_T(T) = \left(11.4 + \frac{T(°C)}{129}\right) \times 10^{-6}$$

According to Hooke's law the axial strain due to an applied stress σ can be expressed as

$$10. \quad \varepsilon_\sigma = \frac{\sigma}{E}$$

where E is the elastic modulus of the material. For steel E in MPa can be expressed as a function of the temperature T as

$$11. \quad E(T) = \left(21.4 + \frac{T(°C)}{175}\right) \times 10^4$$

The equilibrium of forces includes the frictional force between the pipe and the soil presented in (1) as F_R. The pipe internal pressure p also induces a force along the pipe F_p due to the internal fluid pressure.

$$12. \quad F_p = p\frac{\pi d_i^2}{4}$$

There is also an elastic reaction force of the soil F_{el} against the pipe axial movement at the end where the maximum axial displacement occurs. The soil reaction is actually on the following pipe which is perpendicular or in angle after the corner or elbow. This reaction force is not so easy to calculate since it corresponds to a passive earth pressure applied on an unknown surface, probably with a triangular distribution (looking from above). To simplify the calculation F_{el} is assumed to be 20% of $F_R L$:

$$13. \quad F_{el} = 0.2 F_R L$$

Therefore, the total axial strain can be expressed as the sum of the axial strain caused by a change in temperature and due to the forces applied on the pipe by the soil and internal fluid.

$$14. \quad \varepsilon(x) = \alpha_T \Delta T + \frac{\sigma}{E} = \alpha_T \Delta T + \frac{-F_R(L - x) + F_p(1 - 2\nu) - F_{el}}{EA_s}$$

$\Delta T = T - T_0$ is the temperature increase between the temperature under working conditions of heat distribution T and the initial temperature, for instance, during the installation of the pipes T_0. L is the pipe length, x is the distance from a pipe fixed point to the other extreme in a corner for example and v is the Poisson ratio, which has a value of 0.3 for steel. The axial displacement u of the pipe can then be determined by integrating the axial strains due to temperature increase of the fluid carried by the pipe and the strains due to normal and internal stresses on and inside the pipe.

$$15. \quad u(x) = \varepsilon(x)\mathrm{d}x = \left[\alpha_T \Delta T + \frac{F_p(1 - 2\nu) - F_{el}}{EA_s}\right]x - \frac{F_R}{EA_s}\left(Lx - \frac{x^2}{2}\right)$$

REFERENCES

Achmus M (1995) *Zur Berechnung der Beanspruchungen und Verschiebungen Erdverlegter Fernwärmeleitungen. (Calculation of Stresses and Displacements of Underground District Heating Pipelines.)* PhD thesis, Leibniz University of Hanover, Germany (in German).

Achmus M and Rizkallah V (1997) The interaction between underground district heating pipelines and the surrounding soil. *Proceedings of the International Conference on Soil Mechanics and Foundation Engineering, Hamburg, Germany* (Wittke W (ed.)). A.A. Balkema, Rotterdam, the Netherlands, vol. 2, pp. 943–946.

Achmus M and Weidlich I (2016) Interaktion zwischen fernwärmeleitungen und dem umgebenden boden. (Interaction of district heating pipelines and the surrounding soil.) *Bautechnik* **93(9)**: 663–671 (in German).

AGFW (2017) *EnEff: Wärme Einsatz Fliessfähiger Verfüllstoffe zur KMR-Verlegung. Forschung und Entwicklung. (Use of Flowable Fill Materials for the Installation of KMR. Research and Development.) Heft 43*. AGFW, Frankfurt am Main, Germany (in German).

AGFW (2020) *EnEff: Wärme – Technische Gebrauchsdaueranalyse von Wärmenetzen Unter Berücksichtigung Volatiler Energien TGdA – Teil 1: Untersuchungsergebnisse zur Materialdegradation. Heft 55*. AGFW, Frankfurt am Main, Germany (in German).

AGFW (2021) *FW 401: Installation and Calculation of Preinsulated Bonded Pipes for District Heating Networks. Part 10: Static Design; Basics of Stress Analysis*. AGFW, Frankfurt am Main, Germany.

Burd HJ, Beuckelaers WJ, Byrne BW *et al.* (2020) New data analysis methods for instrumented medium-scale monopile field tests. *Géotechnique* **70(11)**: 961–969.

CEN (European Committee for Standardization) (2019) *EN 13941: District Heating Pipes – Design and Installation of Thermal Insulated Bonded Single and Twin Pipe Systems for Directly Buried Hot Water Networks: Part 1: Design. Part 2: Installation*. European Committee for Standardization, Brussels, Belgium.

CEN (2020a) *EN 253: District Heating Pipes: Preinsulated Bonded Pipe Systems for Directly Buried Hot Water Networks: Pipe Assembly of Steel Service Pipe, Polyurethane Thermal Insulation and Outer Casing of Polyethylene*. European Committee for Standardization, Brussels, Belgium.

CEN (2020b) *EN 448: District Heating Pipes: Preinsulated Bonded Pipe Systems for Directly Buried Hot Water Networks: Fitting Assembly of Steel Service Pipe, Polyurethane Thermal Insulation and Outer Casing of Polyethylene*. European Committee for Standardization, Brussels, Belgium.

DIN (2002) *18137-3: Soil, Investigation and Testing: Determination of Shear Strength. Part III: Direct Shear Test*. Beuth Verlag, Berlin, Germany (in German).

Dunnicliff J (2012) *Types of Geotechnical Instrumentation and Their Usage. Chapter 95*. ICE Manual of Geotechnical Engineering, London, UK.

Frederiksen S and Werner S. (2013) *District Heating and Cooling*. Studentlitteratur, Lund, Sweden.

Gerlach T and Achmus M (2017) On the influence of thermally induced radial pipe extension on the axial friction resistance. *Energy Procedia* **116**: 351–364.

Glötzl (2007) *Kunststoff – Stangenextensometer Kompaktausführung für Tunnel und Kavernen. Typ: GKTE 16, Art.-Nr.: 60.10*. Glötzl Baumesstechnik, Rheinstetten, Germany (in German).

Hay S, Villalobos FA, Weidlich I and Wolf I (2018) Analyses of axial displacement measurements from a monitored district heating pipeline system. *Energy Procedia* **149**: 84–93.

Kavvadas MJ (2003) Monitoring and modelling ground deformations during tunnelling. *11th FIG Symposium on Deformation Measurements, Santorini, Greece* (Stiros SC and Pytharouli S (eds)). Patras University, Patras, Greece, pp. 371–390.

Laajalehto T, Kuosa M, Makila T, Lampinen M and Lahdelma R (2014) Energy efficiency improvements utilising mass flow control and a ring topology in a district heating network. *Applied Thermal Engineering* **69(1–2)**: 86–95.

Lund H, Werner S, Wiltshire R *et al.* (2014) 4th Generation District Heating (4GDH): integrating smart thermal grids into future sustainable energy systems. *Energy* **68**: 1–11.

Rohr2 (2017) *Program System for Static and Dynamic Analysis of Complex Piping and Steel Structures*. SIGMA Ingenieurgesellschaft mbH, Unna, Germany (rohr2.com).

sisKMR (2016) District heating pipe stress analysis software. Version 24.9.0. GEF Ingenieur AG, Leimen, Germany (siskmr.com).

Villalobos F, Hay S and Weidlich I (2018) Monitoring in a district heating pipeline system. *International Symposium on Energy Geotechnics SEG-2018* (Ferrari, A. and Laloui, L. (eds)). Springer Series in Geomechanics and Geoengineering, Cham, Switzerland, pp. 132–139.

Villalobos FA, Hay S, Weidlich I and Wolf I (2019) Design, construction and operation of a monitored district heating pipeline system. *Journal of Pipeline Systems Engineering and Practice* **10(3)**: 04019018.

Vulliet L, Casanova N, Inaudi D, Osa-Wyser A and Vurpillot S (1997) Development of fiber optic extensometers. *XIV International Conference on Soil Mechanics and Foundation Engineering, Hamburg, Germany* (Wittke W (ed.)). A.A. Balkema, Rotterdam, the Netherlands, vol. 3, 1527–1530.

Weidlich I (2008) *Untersuchung zur Reibung an Zyklisch Axial Verschobenen Erdverlegten Rohren. (Investigation of Friction on Cyclically and Axially Displaced Buried Pipes.)* PhD thesis, Leibniz University of Hanover, Hanover, Germany (in German).

Weidlich I and Achmus M (2008) Measurement of normal pressures and friction forces acting on buried pipes subjected to cyclic axial displacements in laboratory experiments. *Geotechnical Testing Journal* **31(4)**: 334–343.

Werner S (2017) International review of district heating and cooling. *Energy* **137**: 617–631.

Wolf I, Weidlich I, Nielsen HJ and Hay S (2016) *Langzeitmessstelle Chemnitz – Konzeptbeschreibung und Kostenschätzung. (Long-Term Measurements at Chemnitz – Concept Description and Cost Estimations.) Internal Report*. AGFW, Frankfurt am Main, Germany (in German).